

## Article

# Study of Microwave-Active Composite Materials to Improve the Polyethylene Rotomolding Process

Giorgio Luciano , Maurizio Vignolo, Elisabetta Brunengo, Roberto Utzeri and Paola Stagnaro Istituto di Scienze e Tecnologie Chimiche “Giulio Natta”—SCITEC, National Research Council of Italy,  
Via de Marini 6, 16149 Genova, Italy

\* Correspondence: giorgio.luciano@cnr.it

**Abstract:** The present paper reports on the formulation and characterization of composite coating materials susceptible to microwave (MW) heating to investigate their application in making the rotomolding process (RM) more energy efficient. SiC, Fe<sub>2</sub>SiO<sub>4</sub>, Fe<sub>2</sub>O<sub>3</sub>, TiO<sub>2</sub> and BaTiO<sub>3</sub> and a methyl phenyl silicone resin (MPS) were employed for their formulations. Experimental results showed that the coatings with a ratio of 2:1 *w/w* of inorganic/MPS are the most MW-susceptible materials. To test the coatings in working mimicking conditions, they were applied to molds, and polyethylene samples were manufactured by MW-assisted laboratory uni-axial RM and then characterized by calorimetry, infrared spectroscopy and tensile tests. The results obtained suggest that the coatings developed can be successfully applied to convert molds employed for classical RM process to MW-assisted RM processes.

**Keywords:** rotomolding; microwave heating; microwave-active materials; polyethylene processing

## 1. Introduction

World is implementing sustainable manufacturing and the consequence of effective utilization of resources is increasing productivity. Among the several ways of improving resource effectiveness is avoiding use of resources in the first place and reducing its footprint is paramount [1]. Plastic industry is an energy-intensive one requiring a high volume of electric power for thermal energy where energy use accounts for 5–10% of total production cost [2].

Among the plastic processing methods, rotational molding, also known as rotomolding (RM), is a casting and molding technique useful to produce hollow plastic items of medium to large size [3–5] and involves manufacturing in food and agriculture sector, industrial application, automotive, containers, consumer items and toys. RM is a relatively small part of the plastics industry practiced by approximately 2500 companies around the world. It consumes approximately 0.7% of the total volume of the world production of plastics [6–9] and references therein. To enhance the energy performance of the RM process, the setup required for heating the molds represents a key factor.

In the present paper we focused on enhancing the performance of the process by heating via microwave (MW) irradiation in alternative to using gas or electric ovens. For this aim, we formulated composite materials based on MW-susceptible inorganic compounds (MWSIC) and a methyl phenyl silicone resin to modify conventional RM molds.

In MW heating, also known as dielectric heating, we have a direct transfer of energy (which travels at the speed of light). Consequently, a large amount of power can be saved as well as process times and operational space, considering the physical phenomena involved in the thermal conduction, which is inversely proportional to the square of the distance in the between of the energy source and material to be mold [10].

MW heating is obtained by irradiating active materials in the microwave energy range ( $10^{-3}$  kJ/mol), which is too low of a value for chemical bonds cleavage, but it is sufficient



**Citation:** Luciano, G.; Vignolo, M.; Brunengo, E.; Utzeri, R.; Stagnaro, P. Study of Microwave-Active Composite Materials to Improve the Polyethylene Rotomolding Process. *Polymers* **2023**, *15*, 1061. <https://doi.org/10.3390/polym15051061>

Academic Editor: Markus Gahleitner

Received: 18 November 2022

Revised: 2 February 2023

Accepted: 16 February 2023

Published: 21 February 2023



**Copyright:** © 2023 by the authors. Licensee MDPI, Basel, Switzerland. This article is an open access article distributed under the terms and conditions of the Creative Commons Attribution (CC BY) license (<https://creativecommons.org/licenses/by/4.0/>).

to heat or melt the material by conversion of electromagnetic energy of MW into thermal energy (vibrational motions of chemical bonds). For this reason, the involved materials need to have permanent dipoles (dielectric material) to work well.

In this study, attention was focused on the investigation of MW-active coating materials to be adopted to make the molds suitable for MW heating and thus make it possible to manufacture objects in polyethylene (PE), which is not a dielectrically active material.

Several formulations based on MWSIC were tested in terms of their response to MW irradiation. Measurements of electric power absorbed by selected composite formulations during the imposed microwave cycle were performed and compared to the power needed for corresponding resistive irradiation. PE samples were prepared by MW-assisted uni-axial rotomolding in a lab oven and their properties compared to those of commercial or differently prepared samples.

## 2. Materials and Methods

### 2.1. Materials

Five different MWSIC materials in powder form, namely, silicon carbide (SiC), iron (II) silicate ( $\text{Fe}_2\text{SiO}_4$ ), iron (III) oxide ( $\text{Fe}_2\text{O}_3$ ), titanium (IV) oxide ( $\text{TiO}_2$ ), barium titanate (IV) ( $\text{BaTiO}_3$ ), were tested. Furthermore, it was studied also the effect of different grain size: 35  $\mu\text{m}$  (Fine) and 70  $\mu\text{m}$  (Coarse) for SiC (SCF and SCC, respectively) and 35  $\mu\text{m}$  (Fine) and 500  $\mu\text{m}$  (Coarse) for  $\text{Fe}_2\text{SiO}_4$  (ISF and ISC) (see Table 1).

**Table 1.** List of MW-susceptible inorganic compounds (MWSIC) investigated in this work.

| MWSIC Formula             | Labeled As | Description  |
|---------------------------|------------|--|
| SiC                       | SCF        | Silicon carbide 35 $\mu\text{m}$ grain size            |
| SiC                       | SCC        | Silicon carbide 70 $\mu\text{m}$ grain size            |
| $\text{Fe}_2\text{SiO}_4$ | ISF        | Iron silicate 35 $\mu\text{m}$ grain size              |
| $\text{Fe}_2\text{SiO}_4$ | ISC        | Iron silicate 500 $\mu\text{m}$ grain size             |
| $\text{Fe}_2\text{O}_3$   | IO         | Iron oxide powder < 5 $\mu\text{m}$ , $\geq 99\%$      |
| $\text{TiO}_2$            | TO         | Titanium oxide $\geq 99\%$                             |
| $\text{BaTiO}_3$          | BTO        | Barium titanate powder < 3 $\mu\text{m}$ , $\geq 99\%$ |

Except for ISF and ISC kindly supplied by Slide S.r.l. (Italy), all other inorganic materials were purchased from Sigma-Aldrich (now Merck). Grain size of each substance was obtained from the corresponding label on the commercial container.

To select the most effective materials, that are most capable of efficiently absorbing the MW irradiation heat transfer measures were performed on pelletized samples (discs of 1.2 mm diameter and 0.5 mm thickness) prepared by mixing each MWSIC powder typology with a high-temperature-resistant methyl phenyl silicone resin (MPS). The resin used for the pellet formulation was a commercial two-component silicone elastomer resin (BLUESIL ESA 7252 A&B Italy), fast curable at r.t. and endowed with outstanding flame resistance and good thermal conductivity. The MWSIC powder:MPS resin ratio used was 2:1 ( $w/w$ ).

To gather more information about the materials which can be used as molds, different cylindrical containers were coated with the MW-active composite materials. Aluminum (AL, 50 g), stainless steel (SS, 70 g) and glass (GL, 170 g) containers were tested.

A commercial PE grade (Plastene R210, Polioplast S.p.A. Italy, kindly supplied by Slide S.r.l.) in form of powder (mean dimension 410  $\mu\text{m}$ ), was employed for the tests in lab. Plastene R210 has melt flow index (ISO 1133, 190  $^\circ\text{C}$ , 2.46 kg) 6.25 g/10 min and density 0.936 g/cm<sup>3</sup> (ISO 1183).

For de-molding of PE objects TECNOSIL 21 (SOL TECNO S.r.l., Italy), a technical silicone oil employed in industrial production, was used as detaching agent.

For comparison purposes, two other polyethylene types, namely, Riblene and Kartell jar, were tested by mechanical tensile tests, DSC and ATR-FTIR.

## 2.2. Methods

For the MW-assisted RM process we used a mold coated with MW-susceptible material while in the conventional RM process the mold was uncoated.

A MW oven SAMSUNG M/O 20LT GE71A of 20 L in volume as internal space, operating at 2.45 GHz frequency and at 750 W in power consumption, also equipped with a grill (1100 W in power consumption), was used in heating cycles both with the microwave and the resistance irradiation, for comparison purpose.

To have more information about electric energy saving, the same process parameters (rpm, time, PE powder amount and mold) were adopted to simulate a PE molding using MW irradiation or the resistance of the oven (grill). In each process the absorbed electric current (I) was measured, as well as the voltage value (V) by a digital multimeter (Powermeter GBC KDM-360CTF), respectively, connected to the circuit in series as a galvanometer or in parallel mode as a voltmeter.

The heat transfer measurements were performed positioning each composite pellet on the center of a Teflon plate fixed to the motor axis of the MW oven; the heating cycle was tested at 750 W power both for 5 and 1.5 min.

After the MW irradiation, each pellet was immediately quenched into 20 g of demineralized water at room temperature contained in a plastic Petri with a stirring bar under movement. A Hg thermometer ( $\pm 0.5$  °C in sensibility) was adopted for the temperature measurements.

The composite pellets were rapidly transferred from MW oven to water using high-temperature-resistant and low-thermal-conductivity plastic tweezers.

Microwave-active ISC powder was then chosen as the most suitable to prepare the coatings to be adhered to the molds using the same weight ratio (2:1 powder:resin) previously used for the testing pellets (in this case, 60 g ISC:30 g MPS).

The molding process of PE was tested by performing MW heating cycle of 300 W for 13 min, with a uni-axial rotational movement on the mold axis and a speed of 2 rpm. This speed, as well as the rotation of the mold even during the cooling phase, was possible by replacing the original oven motor (6 rpm). Such a low rotational speed was useful to have sufficient contact time between PE powder and the hot mold internal surface and thus improve the heat exchange.

For each test, 15 g of PE powder were utilized.

Uni-axial tensile measurements on produced PE objects and reference PE counterparts were performed with a Shimadzu ASG-X 10 kN universal machine operating at r.t. on 5 dog-bone specimens (for each PE type) prepared in shape and dimension as requested by ISO 527 (1–5) using a dog-bone shaped mold or a die cut from a previously die-cast PE plate.

To obtain the dog-bone test specimens from uni-axial RM process assisted by MW, a cylinder of PE was prepared from Plastene powder by applying a MW cycle of 10 min at a power energy of 750 W, and a cooling time of about 30 min at a speed of 6–8 °C/min was adopted.

As a first term of comparison, a PE plate was prepared from the same Plastene powder using a Colling press (Laboratory Platen Type P200 bar) and applying the following thermal cycle: heating up to 300 °C, heating rate 10 °C/min, 10 min isothermal at 100 bar, cooling rate at 10 °C/min to room temperature. As a second term of comparison, a commercial PE item, namely, a Kartell PE jar (1000 mL), was employed.

FTIR spectra of PE samples (commercial and rotomolded) were recorded using a Perkin Elmer FTIR Spectrum Two™ spectrophotometer. FTIR spectra were acquired in attenuated total reflection (ATR) mode in the range of 4000–400  $\text{cm}^{-1}$ .

Calorimetric analysis was performed with a DSC Mettler 821° instrument on specimens of 10 mg (cut from the manufactured samples) applying a heating–cooling–heating cycle in the range 100–240 °C under N<sub>2</sub> and at a scan rate of 10 °C/min (EN ISO 11357-1-3).

The morphology and elemental analysis of different MW-active coating formulations were performed by scanning electron microscope (SEM) equipped with a probe for energy-dispersive X-ray analysis (EDX); in detail, it is a HITACHI TM3000 benchtop SEM (15 kV).

### 3. Results and Discussion

The main objective of the present study is to prove the easiness of the conversion of the molds employed in a standard oven to the new coated ones for the MW-assisted RM process. For this purpose, we tested (by heat transfer measurements) the ISC/resin (2:1 ratio) composites on molds made of different materials.

Silicone elastomer resin was chosen due to the working temperature conditions ranging from ambient temperature to 400 °C. It is well established that silicon resins over a wide range of temperatures and they also acknowledged for their fire resistance properties. Moreover, the elastomeric nature of MPS leads to good adherence of the coatings to the molds.

The MWSIC materials of this study were chosen for their dielectric constant (relative permittivity  $\epsilon_R$ ) and dissipation factor values acquired from the literature and reported in Table 2 for room temperature [8–21] and considering negligible the change in value for frequencies higher than 100 MHz [15].

**Table 2.** Literature dielectric data of the MW-susceptible inorganic compounds investigated as suitable materials for molds coating in MW-assisted RM and of other reference materials.

| Material                                 | Measure at          | Dielectric Constant ( $k'$ ) | Dielectric Loss ( $k''$ ) | Loss Tangent ( $k''/k'$ ) |
|--|---------------------|------------------------------|---------------------------|---------------------------|
| Fe <sub>2</sub> SiO <sub>4</sub> [15,16] | 25 °C, 10 GHz       | 5.77                         | 0.01 **                   | 0.0018                    |
| SiC [12]                                 | 25 °C, 3–10 GHz     | 10–60                        | 0.01–36 **                | 0.001–0.58                |
| TiO <sub>2</sub> [11–14]                 | 20/25 °C, 4 GHz     | 80–170                       | 0.008–0.017 **            | 0.0001                    |
| Fe <sub>2</sub> O <sub>3</sub> [17]      | 20/25 °C, 3 GHz     | 6–50                         | 1–4                       | 0.2–0.6                   |
| BaTiO <sub>3</sub> [21]                  | 30 °C, 1 MHz        | 2200                         | 150                       | 0.068 **                  |
| H <sub>2</sub> O [12]                    | 20 °C, 0.1/2.5 GHz  | 78.1/80.1                    | 3.6                       | 0.016/0.123               |
| SiO <sub>2</sub> [12,20]                 | 25 °C, 8.5 GHz      | 3.5–4                        | 0.0008 **                 | 0.0002                    |
| Na <sub>2</sub> SiO <sub>3</sub> [16,17] | 25 °C, 8.5 GHz      | 5.84                         | 0.041 **                  | 0.0070                    |
| PE [12,20]                               | 25 °C, 2.5 GHz      | 2.444                        | 0.002 **                  | 0.0010 (2.6 *)            |
| PVC [12,20]                              | 30 °C, 0.01/2.5 GHz | 3/2.666                      | 0.018/0.04                | 0.001/0.013               |
| PTFE [22]                                | 25 °C, 8.5 GHz      | 2.058                        | 0.0022 **                 | 0.00108                   |
| Silicon RTV 521                          | 23 °C, 8.5 GHz      | 3.31                         | 0.085 **                  | 0.0257                    |

\* Van der Graaff irradiated sample; \*\* valued by Equation (5).

Dielectric constant  $k'$  (and permittivity) and dissipation (loss) factor are related by Equation (1).

$$k^* = k' - jk'' \quad (1)$$

In addition,

$$k' = \epsilon'/\epsilon_0 \quad (2)$$

and

$$k'' = \epsilon''/\epsilon_0 \quad (3)$$

where the terms  $\epsilon'$  and  $\epsilon''$  represent, respectively, the real and imaginary part of complex permittivity  $\epsilon^*$  and  $\epsilon_0$  is the vacuum permittivity.

Because  $k'$  can be related to the material capability to storage electrical energy and  $k''$  represents its capability to dissipate electrical energy, we can define the ability of a material to convert the microwave radiation into heat as the tangential loss ratio:

$$\tan \delta = \varepsilon'' / \varepsilon' \quad (4)$$

Reference materials used in the experiment and the relative parameters for water, PVC, glass, and PTFE are reported in Table 2.

Because the literature data referred to different measurement parameters, such as temperature, frequency, shape, size and so on, heat transfer measurements were here performed in order to establish the response of the chosen compounds in the laboratory environment.

The values of heat exchanged  $Q$  of compounds pelletized with the silicone resin were calculated using Equation (5) and are reported in Table 3.

**Table 3.** Transferred heat calculated with Equation (5).

| MW-Active Compound | Q [J] in Cycle at:<br>750 W, t = 5 min | Q [J] in Cycle at:<br>750 W, t = 1.5 min |
|--------------------|--|--|
| ISC                | 1000                                   | 125                                      |
| ISF                | 700                                    | 84                                       |
| SCC                | 505                                    | 63                                       |
| SCF                | 500                                    | 65                                       |
| TO                 | 170                                    | 75                                       |
| IO                 | 330                                    | 117                                      |
| BTO                | 170                                    | 84                                       |
| IO:BTO (1:1)       | 167                                    | 84                                       |

The amount of heat ( $Q$ ) was estimated by Equation (5)

$$Q = m \cdot c \cdot (\Delta T) \text{ [J]} \quad (5)$$

where  $\Delta T$  is the difference between the temperature value of the water before and after immersion of the pellet,  $m$  correspond to the mass of water and  $c$  is its specific heat value ( $4.18 \text{ J} \cdot \text{g}^{-1} \cdot \text{K}^{-1}$ ). Irradiation time was checked using a precision chronometer.

The results indicate the higher response (expressed as exchanged heat between the material and water used as reference) was obtained by ISC/F samples, followed by SCC/F and IO. The role of the graininess in the response was evaluated both for iron silicate and silicon carbide. In the first case, a difference of 30% in the particles dimension caused a 30% difference in exchanged heat. For the silicon carbide, no effect was found due to the graininess (fine or grain silicon carbide gave identical results).

Among the main objectives of the project one of the most important was the easiness of the conversion of the molds employed in a standard oven to the new coated ones for the MW-assisted RM process. For this purpose, we tested (by heat transfer measurements) the ISC/MPS (2:1 ratio) composites on different materials used for the molds, namely, aluminum, stainless steel and glass (here labeled AL, SS and GL, respectively).

Absorbed power ( $P_{\text{abs}}$ ) was calculated in W units with Equation (6), where  $V$  is the voltage and  $I$  the electric current, converted into W per hour (Wh) to have a direct comparison, considering the impulse time for MW irradiation and the continuous power adsorption for the resistance irradiation.

$$P_{\text{abs}} = V \times I \text{ [W]} \quad (6)$$

In Tables 4 and 5, the resultant absorbed power values are reported.

**Table 4.** Absorbed power calculations with Equation (6) for the MW irradiation @ 300 W ( $t < 300$  s).

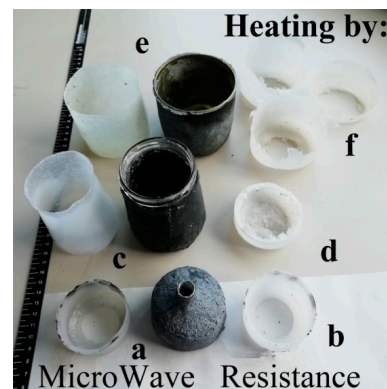
| Mold Material (Time) | Absorbed Current [A] | Grid Voltage [V] | Time [s] | Absorbed Power [Wh] |
|----------------------|----------------------|------------------|----------|---------------------|
| AL (780 s)           | 5.60                 | 225              | 286      | 100                 |
| SS (780 s)           | 5.40                 | 224              | 286      | 96                  |
| GL (780 s)           | 5.70                 | 226              | 286      | 102                 |

**Table 5.** Absorbed power calculations with Equation (6) for the resistance irradiation (780 and 960 s).

| Mold Material (Time) | Absorbed Current [A] | Grid Voltage [V] | Time [s] | Absorbed Power [Wh] |
|----------------------|----------------------|------------------|----------|---------------------|
| AL (780 s)           | 4.00                 | 226              | 780      | 196                 |
| SS (780 s)           | 4.01                 | 224              | 780      | 195                 |
| GL (780 s)           | 4.01                 | 225              | 960      | 241                 |
| GL (960 s)           | 4.03                 | 223              | 780      | 195                 |

All three molds, coated with different materials (AL, SS and GL), reached a maximum temperature of 160 °C under MW and 125 °C when employed under a resistance regime.

The results highlighted that by employing a MW regime, there is the possibility of melting PE and reaching the target temperature for effective RM laboratory processing (as shown in Figure 1).

**Figure 1.** The PE products of molding tests and respective molds (in the between): a, c and e from the MW heating of coated AL, GL and SS molds, respectively; b, d, and f from the resistance heating of the corresponding molds.

Analogous results were obtained for the other materials employed. In all cases, MW-assisted RM ensured a more homogeneous heating of the mold with consequent formation of objects, while the heterogeneous heating obtained by resistance irradiation led to RM-manufactured objects severely failed (missing parts, high surface roughness and residual non-melted raw powder material).

In Table 6, the weights of each PE product in the respective irradiation regime are reported to sustain previous affirmations.

**Table 6.** Weight values of PE products obtained with both MW and Resistive method.

| Material mold | MW Process | Resistive Process |
|---------------|------------|-------------------|
|               | Weight [g] | Weight [g]        |
| SS            | 14.4 (e)   | 13.3 (f)          |
| GL            | 15.0 (c)   | 8.2 (d)           |
| AL            | 15.0 (a)   | 8.2 (b)           |



Reported in Figure 2 are the setups used to study the influence of the geometry of the microwave apparatus on the rotomolding process.

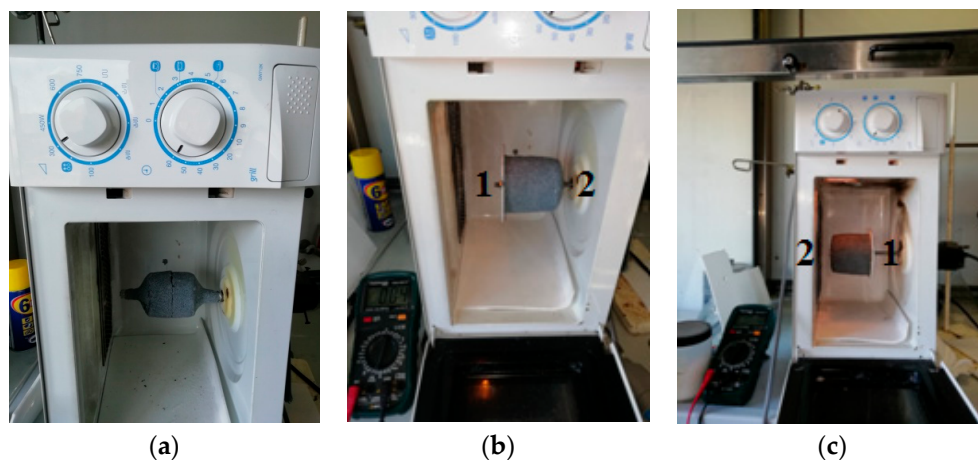


**Figure 2.** Different materials and configurations of molds: (a) AL, (b) GL and (c) SS in different configurations: white PTFE cap (labeled as 1) on the left side or on the right, respectively. The side of the MW-active material is labeled as 2.

Special care should indeed be employed to find the best focus position in the microwave oven in relation to the geometry of the mold, this to avoid unwanted reflection of the waves as they can cause a failure in the manufacturing process (Figure 3).

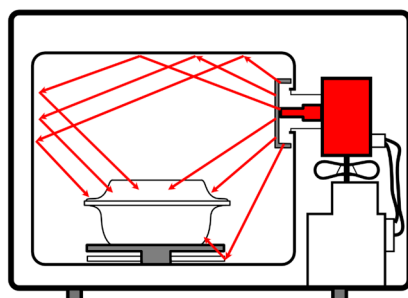


**Figure 3.** Sketch of MW propagation (as red rays) inside the oven. The direction is indicated by red arrows.

Considering the magnetron (i.e., the MW generator) position, we always needed to ensure that the maximum of the reflected radiation could be absorbed by the active material of the mold, as reported in [23,24], while also ensuring the maximum heat exchange in order to ensure the repeatability of the experiments.

The graph in Figure 4 shows the r.t. stress–strain curves obtained by uni-axial tensile measurements corresponding to the most representative samples of the various PE tested. Table 7 summarizes the ensuing tensile data relating to the average values and standard deviation of five specimens for each type of PE investigated.

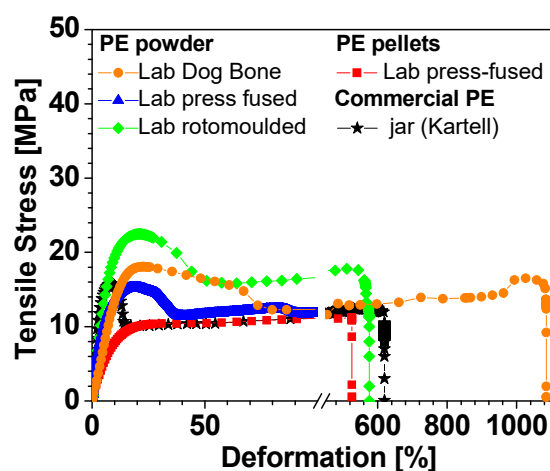


**Figure 4.** Representative stress–strain curves of several PE dog-bone specimens obtained from different processes: cut from commercial PE jar (Kartell 1000 mL), black star; cut from lab press-fused Plastene powder, blue triangle; cut from lab press-fused Riblene pellets, red square; lab press-fused Plastene powder into dog-bone mold, orange circle; cut from lab MW-rotomolded Plastene powder, green diamond.

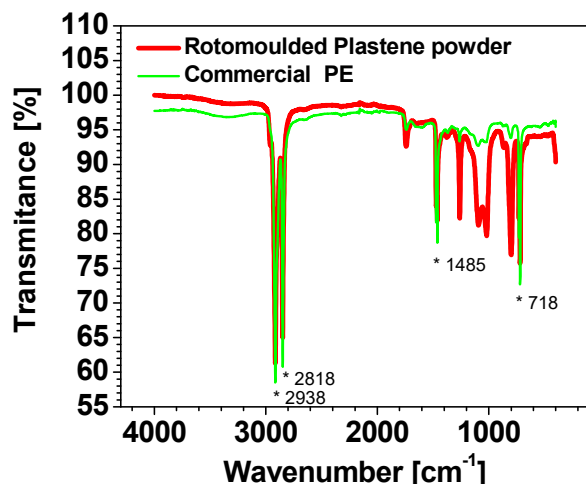
Looking at Figure 4 and Table 7, a very similar behavior can be observed for all the samples. In particular, for the value of strength as well as for the elongation one, both referred at the break. The elongation at the break is more affected by the presence of defects in the structure [25,26], and then some samples break at  $\varepsilon_b$  values less than 200% and others resist until 1100%. The lab MW-rotomolded sample (green diamond) shows a very similar behavior to that of the commercial PE of the Kartell jar (black star). Without going into the details of the results obtained with tensile measurements, as it is beyond the scope of this work, it is possible to conclude that the microwave-assisted rotational molding process, although not yet studied and optimized in detail, proves to be competitive with the classic molding techniques.

**Table 7.** Data from r.t. uni-axial tensile measurements. # denotes the commercial sample is considered as produced by classic molding process, i.e., not using microwave-assisted rotomolding.

| Sample/Preparation Process | Tensile Modulus [MPa] | Tensile Strength at Break [Mpa] | Elongation at Break [%] |
|----------------------------|-----------------------|---------------------------------|-------------------------|
| Riblene (LDPE) [23]        | 120–550               | 32–60                           | 450–810                 |
| Commercial PE/#            | 489 ± 115             | 12.5 ± 1.6                      | 435 ± 178               |
| Press-fused pellets        | 116 ± 12              | 11.6 ± 1.3                      | 520 ± 217               |
| Press-fused powder         | 291 ± 23              | 8.5 ± 2.6                       | 160 ± 80                |
| Lab Dog Bone               | 190 ± 35              | 16. ± 3.4                       | 1100 ± 491              |
| Lab MW-rotomolded          | 287 ± 78              | 21.7 ± 3.2                      | 320 ± 201               |

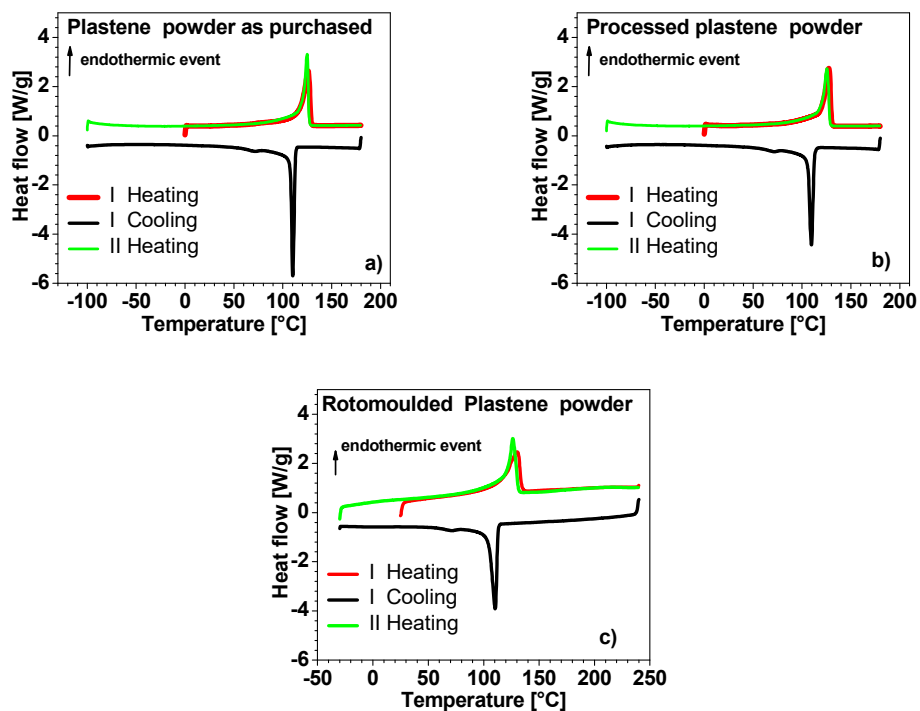
FTIR techniques, as reported by Almond et al. [27], can be used to spot the degradation of the polymer highlighting the presence of groups derived from oxidation (such as carbonyl and hydroxyl groups). In our case, the MW-assisted rotomolding process did not degrade the PE material, as shown (Figure 5) by the absence of the abovementioned groups in the ATR-FTIR spectrum and by its substantial overlapping to that of the commercial PE sample. The only differences, visible between 900 and 1300  $\text{cm}^{-1}$ , are ascribed to the peaks of surface-adhered silicone oil used as de-molding agent [28].





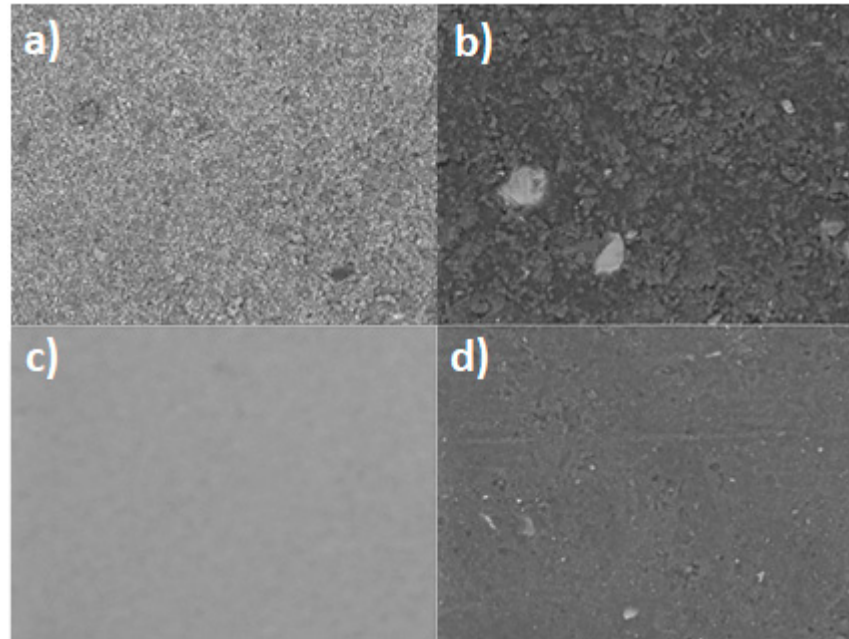
**Figure 5.** ATR-FTIR spectra of MW-rotomolded (red curve) and commercial (green curve) PE samples. The characteristic PE absorbance bands are located at 2914, 2847, 1470, and 718  $\text{cm}^{-1}$  and marked with \*.

Figure 6 show the thermograms resulting from DSC analysis. The canonical peak of PE melting in the interval between (100–135 °C during the I and II heating) is recognized for all the samples in the exam. An analogous observation can be performed for the crystallization peak (centered around 110 °C). No other peaks are present. The values of enthalpy of fusion are comparable (around 150 J/g), again suggesting that no degradation occurred during processing. The high crystallinity degree ( $X_c$  50–52% taking 293  $\text{J g}^{-1}$  as the fusion enthalpy value of a perfect polyethylene crystal) [29,30] of Plastene grade does not permit us to detect the transformation of the amorphous phase from rigid glass and viscous liquid phase ( $T_g = -80$  °C) [30,31].



**Figure 6.** Differential scanning calorimetry graphs relatively to: (a) Plastene powder as purchased, (b) Plastene after press-fusion and (c) MW-rotomolded Plastene.

Furthermore, in order to have more information on the different MW-active coating materials used to cover aluminum, stainless steel and glass molds, each coating material was analyzed by SEM-EDX analysis. In Figure 7, the SEM images of the different MW-active coatings are reported: (a) IO (iron oxide), (b) ISF (iron silicate), (c) TO (titanium oxide) and (d) SCF (silicon carbide). Among the four materials, the iron silicate-based one appears to have a more inhomogeneous surface.



**Figure 7.** SEM images of the dispersion into the silicone resin of (a)  $\text{Fe}_2\text{O}_3$ , (b)  $\text{Fe}_2\text{SiO}_4$ , (c)  $\text{TiO}_2$  and (d)  $\text{SiC}$ .

In Figure 8, the images corresponding to the EDX analysis of the four samples are reported. These confirm the homogeneous dispersion of the powders and their composition. Only the significative elements are reported for each formulation following this order:  $\text{Fe}_2\text{O}_3$ ,  $\text{Fe}_2\text{SiO}_4$ ,  $\text{TiO}_2$  and  $\text{SiC}$ . The formulations are, respectively,

- Fe in (a), (e), (i) and (o);
- Si in (b), (f), (l) and (p);
- Ti in (c), (g), (m) and (q);
- O in (d), (h), (n) and (r).

From EDX images, we can conclude that Si and O are present, as expected, in all the examined composite materials. Ti is obviously present only in (m), while Fe is present in (a) and (e).

Since the melting temperature range of PE is around  $130\text{ }^\circ\text{C}$ , we checked the chemical stability in air of the MW-active coating materials dispersed into the resin matrix in the range temperature between  $0\text{ }^\circ\text{C}$  and  $300\text{ }^\circ\text{C}$  (at the heating and cooling rate of  $10\text{ }^\circ\text{C}/\text{min}$ ) by DSC. All the materials did not show any critical issue.

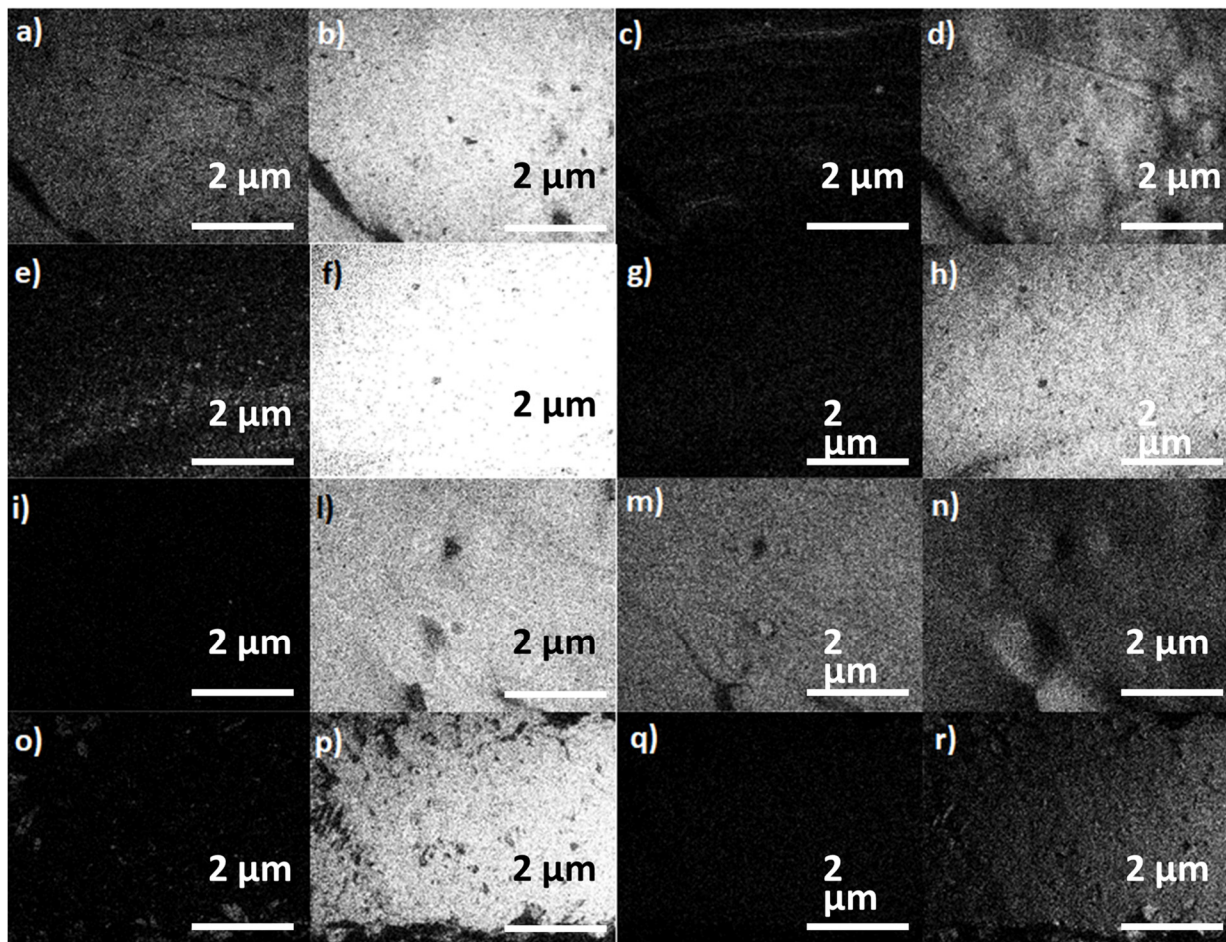


**Figure 8.** Elemental EDX analysis on the four different MW-active materials dispersed into silicone resin matrix: (a) Fe, (b) Si, (c) Ti, (d) O into  $\text{Fe}_2\text{O}_3$ , (e) Fe, (f) Si, (g) Ti and (h) O into  $\text{Fe}_2\text{SiO}_4$ , (i) Fe, (l) Si, (m) Ti and (n) O into  $\text{TiO}_2$ , (o) Fe, (p) Si, (q) Ti and (r) O in to SiC.

#### 4. Conclusions

The focus of this article was the formulation of composite materials responsive to microwave heating as coatings for molds used in the classical rotomolding process to convert it to a microwave-assisted rotomolding technique, thus making the process more efficient.

For this purpose, we used formulates based on a methyl phenyl silicone resin and different inorganic susceptible powders.

The elastomeric material was confirmed to be highly resistant to heat and did not present any degradation during the processes.

The best MW-susceptible inorganic compound used results to be  $\text{Fe}_2\text{SiO}_4$ , followed by SiC and  $\text{Fe}_2\text{O}_3$ , regardless of the material used for the mold (stainless steel, aluminum and glass were tested).

The chemical nature of the composites prepared ensure that in the presence of damage, the composite material can be easily removed or repaired with subsequent additions of new material.

The measurements of the absorbed power reported showed that dielectric heating saves time and energy if compared to the conventional electric resistance heating process.

The results of the tensile test performed according to ISO 527 (1–5) showed the efficiency of the innovative MW-assisted RM process of PE powder, because the performances are comparable to those shown by the commercial PE jar (Kartell) obtained with a classic molding process.

Finally, it should be considered that the MW-RM process is not limited to PE plastic but can be adapted to any plastic or its composite whose molecules do not have a dielectric moment.

**Author Contributions:** Conceptualization, M.V.; methodology, G.L., M.V., E.B., R.U. and P.S.; investigation, M.V., G.L., R.U. and E.B.; resources P.S.; data curation, G.L., M.V. and E.B.; writing—original draft preparation, G.L. and M.V.; writing—review and editing, G.L., M.V., E.B., R.U. and P.S.; supervision, M.V. and P.S.; project administration, P.S.; funding acquisition, P.S. All authors have read and agreed to the published version of the manuscript.

**Funding:** Italian Ministry of Economic Development (MISE), with the contribution of Liguria Region and Lombardy Region.

**Institutional Review Board Statement:** Not applicable.

**Informed Consent Statement:** Not applicable.

**Data Availability Statement:** Data sharing not applicable.

**Acknowledgments:** This work was developed in the framework of ROPEVEMI project (n F/130066/01-05/X38) made possible thanks to co-financing by the Italian Ministry of Economic Development (MISE), Liguria Region and Lombardy Region. We wish to thank the industrial partners involved in the project for their support: Slide S.r.l., Tornova S.r.l., Tecnomodel Engineering S.r.l., Palini Vernici S.r.l.). Warm thanks are due to P. Porta (Slide S.r.l.) for helpful discussion.

**Conflicts of Interest:** The authors declare no conflict of interest.

## References

1. Dornfeld, D.A. Moving towards green and sustainable manufacturing. *Int. J. Precis. Eng. Manuf.-Green Tech.* **2014**, *1*, 63–66. [CrossRef]
2. Khripko, D.; Schlüter, B.A.; Rommel, B.; Rosano, M.; Hesselback, J. Energy demand and efficiency measures in polymer processing: Comparison between temperate and Mediterranean operating plants. *Int. J. Energy Environ. Eng.* **2016**, *7*, 225–233. [CrossRef]
3. Defonseka, C. *Processing Systems for Polymers*; Chapter 8; De Gruyter: Berlin, Germany, 2020; Volume 2020, pp. 65–94.
4. Stampi rotazionali—Tecnomodel. Available online: <https://www.tecnomodel.com/stampi-rotazionali/> (accessed on 12 October 2022).
5. RotoDesign | Tecnologia-Processo. Available online: <http://www.rotodesign.it/tecnologia-processo.html> (accessed on 12 October 2022).
6. Crawford, R.J. Recent advances in the manufacture of plastic products by rotomolding. *J. Mater. Process. Technol.* **1996**, *56*, 263–271. [CrossRef]
7. Ogila, K.O.; Shao, M.; Yang, W.; Tan, J. Rotational molding: A review of the models and materials. *Express Polym. Lett.* **2017**, *11*, 778–798. [CrossRef]
8. Vignali, A.; Iannace, S.; Falcone, G.; Utzeri, R.; Stagnaro, P.; Bertini, F. Lightweight Poly( $\epsilon$ -Caprolactone) Composites with Surface Modified Hollow Glass Microspheres for Use in Rotational Molding: Thermal, Rheological and Mechanical Properties. *Polymers* **2019**, *11*, 624. [CrossRef] [PubMed]
9. Stagnaro, P.; Utzeri, R.; Vignali, A.; Falcone, G.; Iannace, S.; Bertini, F. Lightweight polyethylene-hollow glass microspheres composites for rotational molding technology. *J. App. Polym. Sci.* **2021**, *138*, 49766. [CrossRef]
10. Wypych, A.; Bobowska, I.; Tracz, M.; Opasinska, A.; Kadlubowski, S.; Krzywania-Kaliszewska, A.; Grobelny, J.; Wojciechowski, P. Dielectric Properties and Characterisation of Titanium Dioxide Obtained by Different Chemistry Methods. *J. Nanomater.* **2014**, *2014*, 124814. [CrossRef]
11. Wang, S.T.; Sun, J.; Yu, Y.; Li, Q.J.; Tong, L.; Guo, Y.M.; Wang, C.C. A Facile Method to Increase Dielectric Properties of Rutile TiO<sub>2</sub>. *Ceram. Int.* **2018**. [CrossRef]
12. Hu, W.; Liu, Y.; Withers, R.L.; Frankcombe, T.J.; Norén, L.; Snashall, A.; Kitchin, M.; Smith, P.; Gong, B.; Chen, H.; et al. Electron-pinned defect-dipoles for high-performance colossal permittivity materials. *Nat. Mater.* **2013**, *12*, 821–826. [CrossRef]
13. Available online: <https://www.microwaves101.com/encyclopedias/silicon-carbide> (accessed on 17 October 2022).
14. Sabisky, E.S.; Gerritsen, H.J. Measurements of Dielectric Constant of Rutile (TiO<sub>2</sub>) at Microwave Frequencies between 4.2° and 300 °K. *J. Appl. Phys.* **1962**, *33*, 1450. [CrossRef]
15. Silaghi, M.A. *Chapter 1. Dielectric Material*; IntechOpen: London, UK, 2012. [CrossRef]
16. Chakraborty, S. Frequency-dependent dielectric properties of sodium silicate. *Mod. Phys. Lett. B* **2018**, *32*, 185041. [CrossRef]
17. Chakraborty, S.; Basu, A.; Haldar, S. Effect of doping on dielectric loss of sodium silicate ceramic. *Adv. Sci. Lett.* **2016**, *22*, 21. [CrossRef]



18. Mascia, F.; Fratton, F. Compounds and Compositions for Susceptor Materials. 2011. Available online: <https://patents.google.com/patent/WO2011095883A2/en> (accessed on 17 October 2022).
19. Obarski, G.E. *Wavelength Measurement System for Optical Fiber Communications*; Technical Note NIST-Gov; National Institute of Standards and Technology: Gaithersburg, MD, USA, 1990.
20. Lunt, R.A.; Jackson, A.J.; Walsh, A. Dielectric response of Fe<sub>2</sub>O<sub>3</sub> crystals and thin films. *Chem. Phys. Lett.* **2013**, *586*, 67–69. [[CrossRef](#)]
21. Brunengo, E.; Conzatti, L.; Schizzi, I.; Buscaglia, M.T.; Canu, G.; Curecheriu, L.; Costa, C.; Castellano, M.; Mitoseriu, L.; Stagnaro, P.; et al. Improved dielectric properties of poly(vinylidene fluoride)–BaTiO<sub>3</sub> composites by solvent-free processing. *J. Appl. Polym. Sci.* **2021**, *138*, 50049. [[CrossRef](#)]
22. Opyd, B.; Granat, K.; Nowak, D. Determination of electrical properties of materials used in microwave heating of foundry molds and cores. *Metalurgija* **2015**, *54*, 347–349.
23. Mello, P.A.; Barin, J.S.; Guarnieri, R.A. Chapter 2—Microwave Heating. In *Microwave-Assisted Sample Preparation for Trace Element Analysis*; Elsevier: Amsterdam, The Netherlands, 2014; pp. 59–75.
24. Kamol, S.; Limsuwan, P.; Onreabroy, W. Three-dimensional standing waves in a microwave oven. *Am. J. Phys.* **2010**, *78*, 492–495. [[CrossRef](#)]
25. Mejia, E.; Cherupurakal, N.; Mourad, A.-H.I.; Al Hassanieh, S.; Rabia, M. Effect of Processing Techniques on the Microstructure and Mechanical Performance of High-Density Polyethylene. *Polymers* **2021**, *13*, 3346. [[CrossRef](#)]
26. Osswald, T.A.; Menges, G. Failure and Damage of Polymers. In *Materials Science of Polymers for Engineers*; Carl Hanser Verlag: Munich, Germany, 2012; pp. 423–487. [[CrossRef](#)]
27. Almond, J.; Sugumaar, P.; Wenzel, M.N.; Hill, G.; Wallis, C. Determination of the carbonyl index of polyethylene and polypropylene using specified area under band methodology with ATR-FTIR spectroscopy. *e-Polymers* **2020**, *20*, 369–381. [[CrossRef](#)]
28. Chamerski, K.; Lesniak, M.; Sitarz, M.; Stopa, M.; Filipecki, J. An Investigation of the Effect of Silicone Oil on Polymer Intraocular Lenses by Means of PALS, FT-IR and Raman Spectroscopies. *Spectrochim. Acta Part A Mol. Biomol. Spectrosc.* **2016**, *167*, 96–100. [[CrossRef](#)]
29. Wunderlich, B. *Thermal Analysis of Polymeric Materials*; Springer: Berlin/Heidelberg, Germany, 2005.
30. Sadrabadi, T.E.; Zebarjad, S.M.; Khaki, J.V.; Sahebian, S. On the dependence of avrami indexes of MDPE on milling time. *Polym. Plast. Technol. Eng.* **2010**, *49*, 1284–1288. [[CrossRef](#)]
31. Wu, S.; Zhang, X.; Sun, Y.; Yang, H.; Lin, B.; Han, X.; Chen, P. Study on the influence of crosslinking density and free polysiloxan chain length on oxygen permeability and hydrophilicity of multicomponent silicone hydrogels. *Colloid Polym. Sci.* **2021**, *299*, 1327–1335. [[CrossRef](#)]

**Disclaimer/Publisher’s Note:** The statements, opinions and data contained in all publications are solely those of the individual author(s) and contributor(s) and not of MDPI and/or the editor(s). MDPI and/or the editor(s) disclaim responsibility for any injury to people or property resulting from any ideas, methods, instructions or products referred to in the content.